Research

Topographic distributions of emergent trees in tropical forests of the Osa Peninsula, Costa Rica

Christopher S. Balzotti, Gregory P. Asner, Philip G. Taylor, Rebecca Cole, Brooke B. Osborne, Cory C. Cleveland, Stephen Porder and Alan R. Townsend

C. S. Balzotti (cbalzotti@carnegiescience.edu) and G. P. Asner, Dept of Global Ecology, Carnegie Inst. for Science, Stanford, CA, USA. – P. G. Taylor and A. R. Townsend, Nicholas School of the Environment, Duke Univ., Durham, NC, USA. – R. Cole, Dept of Natural Resources and Environmental Management, Univ. of Hawaii at Manoa, Honolulu, HI, USA. – B. B. Osborne and S. Porder, Dept of Ecology and Evolutionary Biology, Brown Univ., Providence, RI, USA. – C. C. Cleveland, Dept of Ecosystem and Conservation Sciences, Univ. of Montana, Missoula, MT, USA.

Tropical rainforests are reservoirs of terrestrial carbon and biodiversity. Large and often emergent trees store disproportionately large amounts of aboveground carbon and greatly influence the structure and functioning of tropical rainforests. Despite their importance, controls on the abundance and distribution of emergent trees are largely unknown across tropical landscapes. Conventional field approaches are limited in their ability to characterize patterns in emergent trees across vast landscapes with varying environmental conditions and floristic composition. Here, we used a high-resolution light detection and ranging (LiDAR) sensor aboard the Carnegie Airborne Observatory Airborne Taxonomic Mapping System (CAO-AToMS) to examine the abundance and distribution of tall emergent tree crowns (ETC) relative to surrounding tree crowns (STC) across the Osa Peninsula, a geologically and topographically diverse region of Costa Rica. The abundance of ETC was clearly influenced by fine-scale topographic variation, with distribution patterns that held across a variety of geologic substrates. Specifically, the density of ETC was much greater on lower slopes and in valleys, compared to upper slopes and ridges. Furthermore, using the CAO high-fidelity imaging spectrometer, ETC had a different spectral signature than that of STC. Most notably, ETC had lower remotely sensed foliar nitrogen than STC, which was verified with an independent field survey of canopy leaf chemistry. The underlying mechanisms to explain the topographic-dependence of ETCs and linkages to canopy N are unknown, and remain an important area of research.

Large-diameter emergent trees are keystone structures in tropical forest ecosystems (Fichtler et al. 2003, Lindenmayer et al. 2012). At a local scale, they add vertical and horizontal structural complexity to forest canopies, providing specialized microhabitats and food resources for an array of plant and wildlife species (Laurance et al. 2000, Fichtler et al. 2003, Oliveira et al. 2008). At the regional to global scale, these trees provide valuable ecosystem services such as carbon sequestration. Large emergent trees often exist at low densities in tropical forests, yet they make up a disproportionately large amount of the aboveground biomass (AGB; Clark and Clark 1996, Thomas et al. 2013, Sist et al. 2014). For example, Sist et al. (2014) found that in the eastern Amazon, large emergent trees represented only 9% of the tree density but accounted for 49% of the AGB. However, a multitude of factors, such as logging, anthropogenic land use and climate change, are all contributing to their decline (Cochrane and Laurance 2008, Allen et al. 2010, Lindenmayer et al. 2014). Across the tropics, large trees seem to be especially sensitive to water stress, and their mortality has increased as a result of recent and more frequent droughts (Nepstad et al. 2007,

Phillips et al. 2010). Despite their importance and documented decline, the mechanisms describing tropical emergent tree distributions and function are largely unknown.

An emergent must survive within the hypercompetitive and heterogeneous conditions of the rainforest, where pests, pathogens, herbivores, and critical resources (i.e. light, water, soil nutrients) vary across space and time. Once a tree's crown emerges above the surrounding canopy, it encounters unique environmental conditions that ultimately enhance fitness over the costs of added risks (Thomas et al. 2013). Greater light availability may stimulate growth and increase persistence, and increased exposure to windy conditions may enhance seed dispersal from a greater height. At the same time, emergent trees must cope with increased ultraviolet radiation, higher temperatures, wind-induced breakage, and greater water stress on stomata conductance, which could hamper the function of emergent trees (King 1990, Ryan and Yoder 1997, Midgley 2003, Niklas 2007). Despite the challenges associated with growing tall, many trees have evolved to flourish at great heights (Koch et al. 2015, Sillett et al. 2015a, b).

Environmental factors can vary tremendously across topographically diverse landscapes, where landform variation gives rise to spatial patterning of wind stress, light and water availability, as well as soil structure and fertility. Recent landscape-scale investigations suggest that topography influences the distribution and survival of tropical emergent trees at multiple spatial scales (Luizão et al. 2004, Detto et al. 2013, Thomas et al. 2013). Additionally, in our study area (Taylor et al. 2015) and others (Mascaro et al. 2011, Detto et al. 2013), it was found that aboveground biomass reaches maximum levels on slopes (Taylor et al. 2015), though it was unclear if emergent trees, which disproportionately influence aboveground carbon storage, were consistently more common in these areas.

Regardless of mechanism, the morphological and physiological traits of emergent trees are likely attuned to environmental conditions that optimize their survival. Though rarely studied, crowns of older and taller trees of many species have thicker cuticle and palisade layers, and higher amounts of dry mass per unit area (Niinemets et al. 2001, England and Attiwill 2006). These adaptations may increase drought tolerance and defense against irradiation (Niinemets 2002, Kenzo et al. 2012). Studies at small spatial scales, evaluating foliar nutrient concentrations, have found that emergent crowns have reduced amounts of foliar nitrogen (N) compared to trees lower in the canopy (Kenzo et al. 2012). Lower foliar N may reflect a resource-use strategy that optimizes carbon use efficiency and allocation, or reflect proportional investments in defense compounds or other N reallocations, independent of photosynthetic nutrient demands (Reich 2014). Such coordinated tradeoffs in crown traits are reflective of whole organism strategies to survive, which ultimately affect the composition, form and function of the entire ecosystem (Violle et al. 2014).

Landscape-scale studies are rare because of the challenges of mapping emergent trees across large spatial scales with sufficient state factor variation to identify potential environmental filtering (Thomas et al. 2013). Recent advancements in remote sensing platforms, such as the Carnegie Airborne Observatory (CAO; Asner et al. 2012), provide an opportunity to simultaneously evaluate the structure of forests and the chemistry of their canopies at a fine resolution across large areas. Here, we map the distribution of the tallest emergent tree crowns across the Osa Peninsula, Costa Rica to investigate how variation in geology and topography influences the spatial patterning of emergent trees. Specifically, we examine if emergent trees are more prevalent in areas of the landscape where environmental features could maximize their growth and survival. This was accomplished using light detection and ranging (LiDAR) to map variation in tropical forest canopy height in parallel with landscape variation. Second, we examine if foliar N is lower in the tallest emergent crowns compared to the surrounding crowns. This was accomplished with the CAO high fidelity imaging spectrometer (HiFIS). Shifts in canopy N content can offer insight into the life-history strategies of emergent versus surrounding trees. Resolving such linkages will yield insight into the environmental constraints and physiological function of emergent trees, which play a disproportionate role in tropical forest structure and function.

Methods

Study region

The Osa Peninsula is located in southwestern Costa Rica and is home to the largest tract of lowland tropical forest on the American Pacific coastline (Fig. 1). The Osa Peninsula is geologically complex, and topographically varied, with elevation ranging from sea level to 745 m a.s.l. (Buchs et al. 2009, Taylor et al. 2015). According to the Holdridge (1967) life zone classification system, the majority (> 90%) of the peninsula is dominated by tropical wet forest; however, it is also home to premontane wet and tropical moist forests (Cornejo et al. 2012). The Osa Peninsula has generally fertile soils, though nutrient content and physical properties of soils shift with geology and topographic position in the landscape (Wanek et al. 2008, Weintraub et al. 2015), creating edaphic heterogeneity at local to regional scales. This heterogeneity is partially due to high levels of mean annual rainfall (3000 to 7000 mm yr^{-1}; Taylor et al. 2015). The region is characterized by high plant and wildlife diversity and endemism (Barrantes et al. 1999, Wanek et al. 2008). In a recent study of 458 tree species collected on the Osa Peninsula, 4.8% were found to be endemic to the peninsula and 25% were endemic to Central-South Mesoamerica (Cornejo et al. 2012). The Osa Peninsula also contains some of the most carbon-rich forests in the Neotropics, with trees reaching heights over 60 m and aboveground carbon density exceeding 225 Mg C ha^{-1} (Taylor et al. 2015). The region, with its diverse combination of state factors, presents an ideal study area to explore the influence of geology and topography on the distribution of emergent trees.

Within the Osa Peninsula and surrounding areas, five study locations were selected to test if the tallest emergent trees had unique distribution patterns within the landscape (Table 1; Fig. 1, 2). The five study areas capture the four dominant geologic substrates that underlie forests of the Osa Peninsula: Vaquedano Basalt, Golfito Basalt, Miocene Sediments and Pliocene Sediments. Within the Pliocene Sediment formation, two sites in close proximity were chosen on landscapes of differing ages of geomorphological development. See Buchs et al. (2009) and Taylor et al. (2015) for an in depth description of the surrounding geology. Prior to removal of clouds and anthropogenic disturbance, each study area covered roughly 545 ha.

Defining tall crowns

Emergent trees are defined by their taller height, relative to the surrounding stature of the forest canopy. For example, in a tropical wet forest on the Atlantic side of Costa Rica (La Selva), where the mean height is 20.3 m, tall emergent trees were defined as > 40 m (Thomas et al. 2013). The mean height for the Osa Peninsula canopy is nearly 10 m higher, in general, than La Selva (Table 1), so a taller threshold was used. The tallest emergent tree crowns (ETC) were defined here as tree crowns more than one standard deviation taller than the mean height of the forest (> 45 m). For comparison purposes, trees between 10–45 m tall were considered as surrounding tree crowns (STC). Additional canopy height
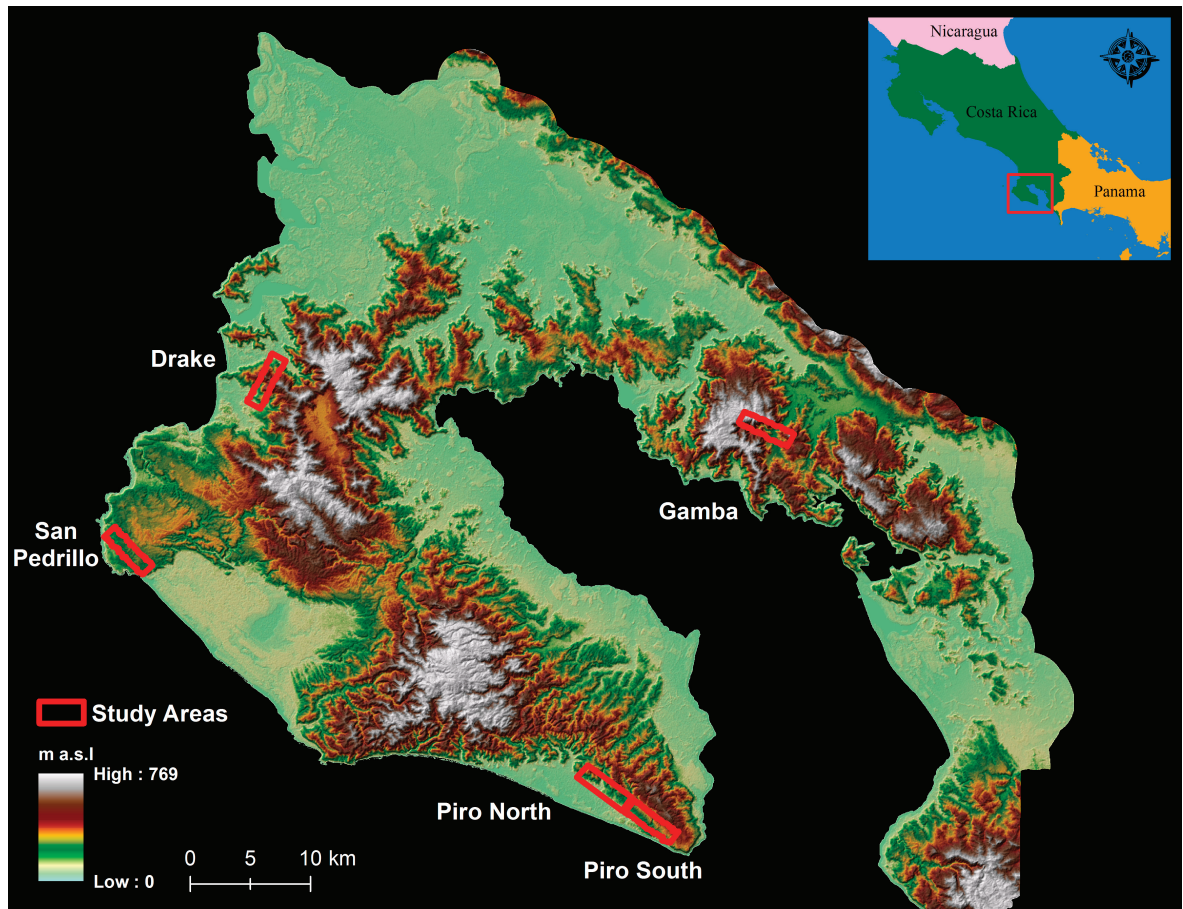
Figure 1. A digital elevation model (from NASA Shuttle Radar Topography Mission data) of the Osa Peninsula, with five study landscapes outlined in red. The inset shows the location of the Osa Peninsula within Costa Rica.

classes were created to compare to the ETC distribution (10–20, 20–30, 30–40 m).

Remotely sensed data

Remotely sensed data were collected in 2012 with the CAO-AToMS platform onboard a Dornier 228 aircraft using two sensors: a high-fidelity imaging spectrometer (HiFIS) and a dual laser, waveform LiDAR (Asner et al. 2012). The LiDAR beam divergence was set to 0.56 mrad for each of the two lasers, allowing for two laser shots m^{-2}. The LiDAR data were used to create highly accurate, 2 m resolution digital elevation models (DEMs) and top-of-canopy height (TCH) models. The performance of the TCH models, within the study area, was validated against field collected data, with a reported root mean square error of 2.49 m (Taylor et al. 2015). To generate the DEM, a 10×10 m kernel was passed over the georeferenced LiDAR data points. The lowest elevation estimate in each kernel was assumed to be ground. The remaining ground points in each kernel were determined by an iterative process of fitting a horizontal

Table 1. Descriptive information about each study landscape. *MAP represents mean annual precipitation between the years 1950–2000. MAT is mean annual temperature for the same time period. Both the MAP and the MAT data were obtained from the WorldClim website May 2015 (<www.worldclim.org>).

| Landscape	Area (ha)	MAP* (mm)	MAT* (°C)	Mean elevation (m a.s.l)	Elevation Range (m a.s.l)	Geology	Mean TCH (>10 m)/STD	Percent canopy cover >45 m
Piro South	535	3525	25.4	134	23–283	Miocene-Pliocene shallow water sediments	32.8/11.0	15.2
Piro North	546	3808	26.1	81	21–242	Miocene-Pliocene shallow water sediments	28.5/9.7	6.2
San Pedrillo	522	4712	25.9	92	15–150	Pliocene Shallow to Offshore Sediment	33/10.1	14.7
Drake	545	4080	25.6	141	17–376	Basalt Vaquedano	30.4/10.9	11.1
Gamba	531	3904	25.8	247	100–516	Basalt Golfito	27.7/9.6	5
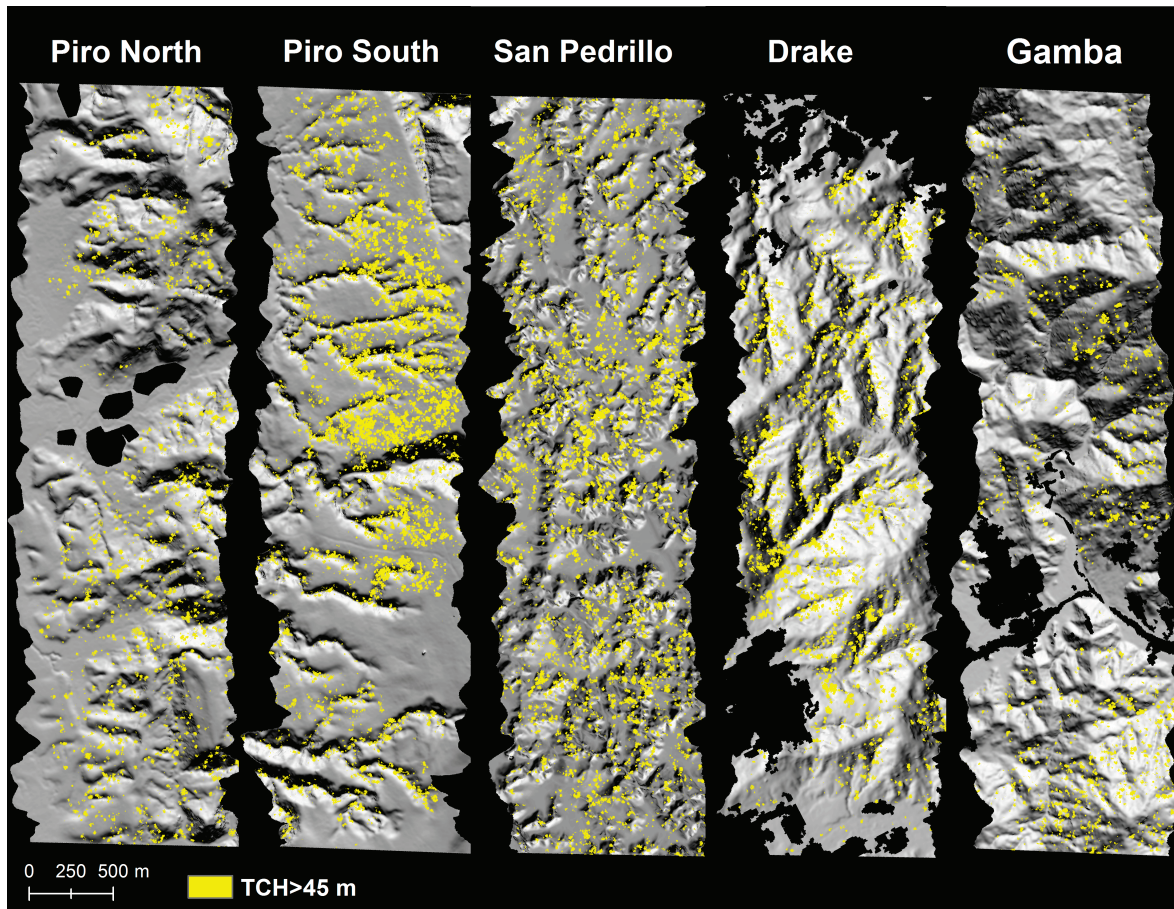
Figure 2. The five study landscapes selected using Carnegie Airborne Observatory (CAO) images of ground topography (gray) and top-of-canopy height (TCH) > 45 m (yellow). From left to right: Piro North, Piro South, San Pedrillo, Drake, and Gamba.

plane and selecting the nearest point that was < 5.5° and < 1.5 m higher in elevation (Asner et al. 2015b). A digital surface model (DSM), representing the outermost layer, was generated using first laser returns from the LiDAR. The vertical difference between the DEM and the DSM yielded the TCH model (Asner et al. 2015b). To reduce the effects of anthropogenic influences, in particular secondary forests, trees < 10 m tall were not considered in this study.

The onboard HiFIS measured spectral radiance in 5 nm increments, with nominally 6 nm spectral response function (bands; full-width at half-maximum), spanning the visible to shortwave infrared spectrum (380–2510 nm). The raw output of the HiFIS was 427 contiguous spectral bands at a resolution of 2 m. Prior to analysis, the HiFIS data were converted from raw digital numbers to atmospherically corrected reflectance. Following conversion, the original 427 HiFIS bands were resampled to 214 bands at 10 nm increments. The number of bands was further reduced for analysis by removing the bands in the range of atmospheric water absorption (1350–1480, 1780–2032 nm) and bands in the far ends of the spectra (< 410 nm, > 2450 nm). The data were then converted to brightness normalized reflectance (Asner et al. 2015a). Brightness normalization minimizes the differences in observed brightness, due to canopy leaf tissue orientation and depth (Feilhauer et al. 2010). The spectral data were then filtered, using a LiDAR HiFIS fusion

technique, to remove bare-ground and canopy shading (Asner et al. 2007). Finally, clouds and cloud shadows were removed manually. See Asner et al. (2015a) for details of the HiFIS preprocessing methods used.

After this extensive pre-screening process, the remaining canopy data were more representative of 'sunlit canopy foliage' (Asner et al. 2015b). Using these 'sunlit canopy foliage' data, spectral profiles for ETC and STC were generated, along with a map of estimated foliar N (%) concentration by mass. The foliar N map was created at the same resolution as the HiFIS data, using a Partial Least Squares Regression (Haaland and Thomas 1988) method described in Asner et al. (2015b). The N map could not be validated here, due to a lack of geospatially located field data, at the time of the flight. However, the model was built and validated using 22 tropical forest types across a 3500 m elevation gradient throughout Peru (Asner et al. 2014, 2015a). Furthermore, an independent foliar nutrient data set collected in 2014 on the Osa Peninsula (described below) was used, for comparison to the remotely sensed canopy N.

Topographic position

The LiDAR-generated DEMs were used to classify the landscape into six slope positions. Before classification, the

DEMs were smoothed to remove small imperfections using the Perona-Malik nonlinear filter, a method optimized for high resolution LiDAR data (Passalacqua et al. 2010). Smoothing was completed using the geomorphic feature extraction tool box 2.0 (GeoNet; Passalacqua et al. 2010), implemented in MATLAB® (MATLAB and Statistics Toolbox Release, The MathWorks, Natick, MA, USA). After smoothing, slope position classes were created using the Land Facet Corridor Designer Toolbox (Jenness et al. 2013), implemented with ESRI software (ESRI 2014. ArcMap® 10.2.2, Redlands, CA). The six topographic classes created were valleys, lower slopes, steep slopes (> 10°), upper slopes, gentle slopes (< 10°) and ridges (Fig. 3).

Field data

In 2014, leaf samples from 107 trees, represented by eight species, were collected from three of the study areas: Piro North, Piro South and Drake (Taylor et al. unpubl.). Tree climbers collected mature leaves from fully sunlit branches located near treetops for each tree. Frozen leaf disks were sent to the Carnegie Spectranomics Laboratory, Stanford, CA, USA, for chemical analysis. Total N was determined on oven-dried, ground samples using a combustion-reduction elemental analyzer (Costec Analytical Technologies, Valencia,

CA, USA). See Asner et al. (2011) for further details of the laboratory protocols used.

Analyses

Statistical analysis was performed using JMP® ver. 12 (SAS Inst., Cary, NC). Differences in distribution patterns across the six topographic classes and all height classes were calculated with contingency tables. A chi-squared test was applied to determine statistical relevance of the observed patterns between ETC and STC. For the contingency tables, all crowns and height classes were used. However, in order to maintain independence for the chi-square test, and not have multiple samples from individual trees, 200 random points from ETC and STC were extracted from each study site. These points were combined for the regional site assessment with a total of 1000 samples per class. A chi-square test was applied to the combined data as well as each individual site.

The mean brightness-normalized spectral profiles (Feilhauer et al. 2010) were extracted from all ETC and STC, using ENVI ver. 4.8 (Exelis Visual Information Solutions, Boulder, CO). The absolute difference between ETC and STC profiles, was used to compare the spectra of the two height classes. For the remotely sensed N, the same sampling strategy as listed above was used for a total of 1000 sample
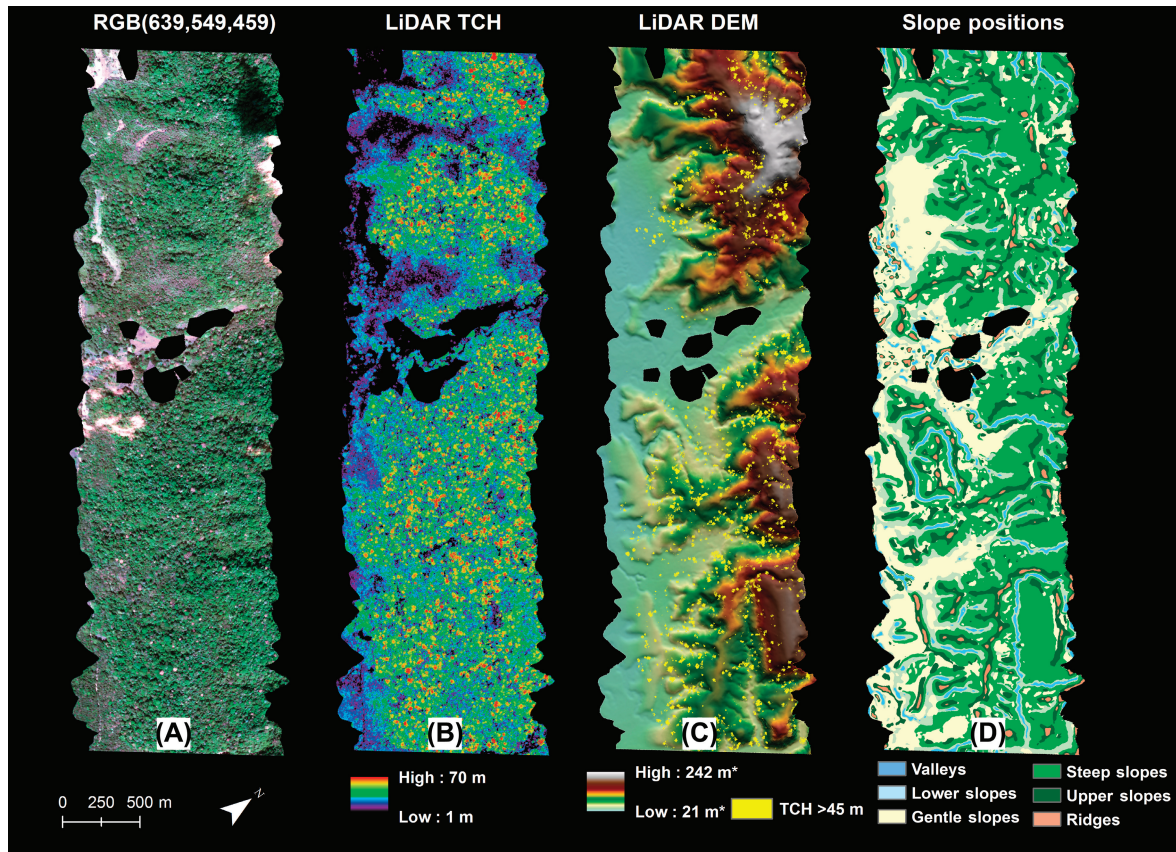

Figure 3. Example of data collected from the CAO for Piro North. (A) Imaging spectroscopy data used to create spectral profiles and foliar N maps. Image shown as false color composite (RGB = 639/549/459 nm). (B) Light Detection and Ranging (LiDAR)-generated top-of-canopy height (TCH). (C) LiDAR-generated digital elevation model (DEM) with TCH > 45 m shown in yellow (* m a.s.l.). (D) Slope positions generated from the LiDAR DEM. Valleys are shown in dark blue, lower slopes in light blue, upper slopes in dark green, steep slopes in green, gentle slopes in tan, and ridges in orange.

points for ETC and STC. A students t-test was performed to determine if there was a statistical difference between the remotely sensed ETC and the STC N. The field collected foliar N data were not normally distributed so a Wilcoxon test was used to compare trees with mean crown height > 45 m to crowns < 45 m.

Results

Patterns in ETC and slope position

Across the Osa Peninsula, very tall emergent trees are relatively rare in the landscape. All study areas combined had an overall ETC cover of 10.5%, with the largest amount found at Piro South (15.2%) and the smallest at Gamba (5%; Table 1). The small amount of ETC cover is consistent with observed values of large diameter emergent trees in other tropical forests, such as the Eastern Amazon (9.3%; Sist et al. 2014). Although the total amount of ETC varied between the study areas, the distribution pattern of ETC remained the same across all study areas and geologic substrates (Supplementary material Appendix 1, Fig. A1). Emergent tree density was higher in valleys and in lower slope reaches (26.78%; Fig. 4) compared to all other height classes (10–20 m, 16.1%; 20–30 m 15.1%; 30–40 m 15.9%; Fig. 4). Furthermore, ETC density was lower on upper slope reaches, gentle slopes and ridges compared to STC (Fig. 4). Using a Chi Square test, comparing the distribution pattern across slope position and landscapes,
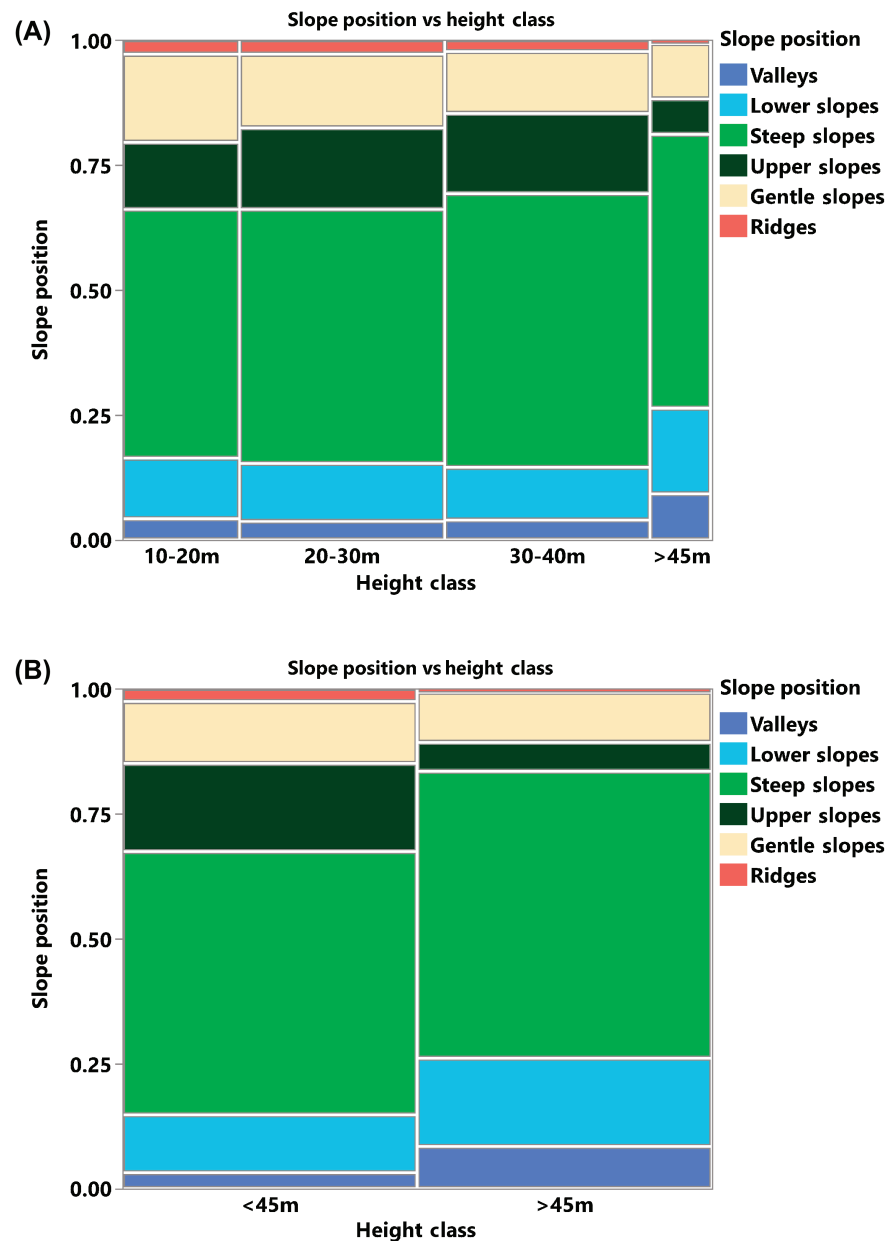

Figure 4. (A) Contingency table showing the distribution frequency of canopy height classes across slope positions across all landscapes, see Supplementary material Appendix 1, Fig. A1 for individual landscape results. (B) Contingency table for random samples comparing tall top-of-canopy > 45 m (ETC) to surrounding top-of-canopy between 10–45 m (STC; X^2 (5, n = 2000) = 106.81, p < 0.0001).

the observed difference between ETC and STC was found to be statistically significant (X^2 (5, n = 2000) = 106.81, p < 0.0001). This same pattern of ETC distribution and statistical relevance was observed at each of the individual study areas as well (Supplementary material Appendix 1, Fig. A1).

Spectral profiles and nitrogen

Brightness-normalized reflectance comparisons between ETC and STC showed clear spectral composition differences in the near infrared (NIR) and the shortwave infrared (SWIR) portions of the spectrum (Fig. 5). ETC had higher reflectance in the NIR and lower reflectance in the SWIR, with the largest differences observed between the wavelengths of 730–920 and 1510–1760 nm. These spectral differences were found in regions associated with N absorption (Fig. 5).

Remotely sensed canopy N, of all landscapes combined, had an estimated ETC N (M = 1.94, SD = 0.58) slightly lower than STC N (M = 2.20, SD = 0.66; Student's t-test, p < 0.001; Fig. 6). The pattern of lower estimated N for the ETC compared to STC held across all landscapes (Supplementary material Appendix 1, Fig. A2). Although Piro North and Piro South were located on the same substrate, and were in very close proximity, Piro North ETC had the highest estimated N (M = 2.0, SD = 0.58) and Piro South had one of the lowest (M = 1.88, SD = 0.54). The independent field data also indicated that the tallest trees had lower N (M = 1.90, SD = 0.54) compared to trees < 45 m (M = 2.20, SD = 0.66, Wilcoxon test p < 0.05), corroborating the remotely sensed results.

Discussion

Topography exerted a strong control on the distribution of emergent trees. Emergent trees were disproportionately common in valleys and lower slopes, and less abundant on ridges and slopes immediately adjacent to ridges. Although the study areas covered four geologic substrates (Table 1), the distribution of the tallest trees followed the same basic pattern across all substrates, suggesting that regional diversity in geologic type and conditions played little role in determining the distribution patterns of emergent trees on the Osa Peninsula, Costa Rica. Furthermore, this landscape-level pattern is consistent with other tropical forests in the region (Detto et al. 2013, Thomas et al. 2013) and implies environmental filtering of ETC abundance and distribution. Topography may control the spatial patterning of emergent trees by creating variation in water availability, soil fertility, disturbance regime, light availability, and species interactions. We explore the potential influence and interaction of these factors on the Osa Peninsula.

Water availability regulates tropical rainforest growth (Schuur and Matson 2001, Del Grosso 2008, Phillips et al. 2010), and topography can strongly influence soil moisture by creating spatial variation in soil depth and textural composition (Whittaker 1972, Newbery and Proctor 1984, Aiba and Kitayama 1999, Takyu et al. 2002). Even on the Osa

Peninsula, where rainfall generally surpasses plant demand on an annual basis (i.e. rainfall > evapotranspiration potential), soil water content is topographically dependent (Hofhansel et al. 2014). Recent research on the Osa Peninsula indicates that C allocation to wood growth is sensitive to topographic variations in soil moisture (Hofhansl et al. 2014). Forests on ridges, which have shallow soils prone to desiccation, are more sensitive to drought stress, experienced during El Niño periods, than ravine forests. Ravine forest soils are deeper and have greater clay and organic matter content, enhancing water-holding capacity, which may underpin greater rates of wood production during drier periods by reducing hydraulic stress (Hofhansl et al. 2014). This notion aligns with recent observations that wood growth increases with greater water availability at both seasonal and interannual timescales (Doughty et al. 2014, Hofhansl et al. 2014, Wagner et al. 2014).

Variations in soil properties along topography gradients can also influence forest dynamics and structure (Tanner 1977, Webb et al. 1999, Takyu et al. 2002, 2003). Shallow, less developed soils on ridges and upper slopes offer less structural stability compared to deeper soils on lower slopes and valleys. Moreover, forests in these landscape positions are exposed to greater wind stress that could enhance the mortality of large trees. The combination of edaphic properties and greater risk of wind disturbance may partially explain why ridge forests are generally shorter, denser and exhibit greater turnover on the Osa Peninsula (Wanek et al. 2008, Hofhansl et al. 2014) and elsewhere (Chen et al. 1997, Webb et al. 1999, Takyu et al. 2002, Homeier et al. 2010).

Topography also affects soil fertility, controlling the distribution of nutrients across the landscape by organizing the geomorphic processes, such as erosion, hydrologic leaching and downslope accumulation (Takyu et al. 2003, Porder et al. 2007, Vitousek et al. 2010). The erosional deposition of bedrock nutrients can enrich slopes with nutrients critical to forest growth (Takyu et al. 2003, Porder et al. 2005). Prior fieldwork in the region (Weintraub pers. comm.) and in other locations (Vitousek et al. 2003) demonstrates that soil phosphorus, often a growth-limiting nutrient in tropical rainforests, is greatest in lower slope areas, where ETCs are abundant. A host of correlative studies suggests that soil P is the best predictor of forest growth (Cleveland et al. 2011, Quesada et al. 2012), which appears in wide regional gradients in canopy P in the Amazon Basin (Fyllas et al. 2009, Asner et al. 2015b). Yet experimental evidence for single nutrient limitation in continental tropical rainforests is seldom tested and very rarely observed (Cleveland et al. 2011, Wright et al. 2011). Instead, multiple nutrients can simultaneously limit tree growth within a forest stand, as limitation can vary by species and tree age (Wright et al. 2011). Thus, while landscape nutrient distribution may play a role, it is unlikely that nutrient limitation of primary productivity alone can explain the abundance of emergent trees in lower slope regions of the Osa peninsula.

Light availability also varies with topographic position, with less available light in the lower slopes compared to ridges and upper slopes (Fladeland et al. 2003, Tateno and Takeda 2003). Gradients in light are often thought to drive growth and competition of temperate and tropical trees
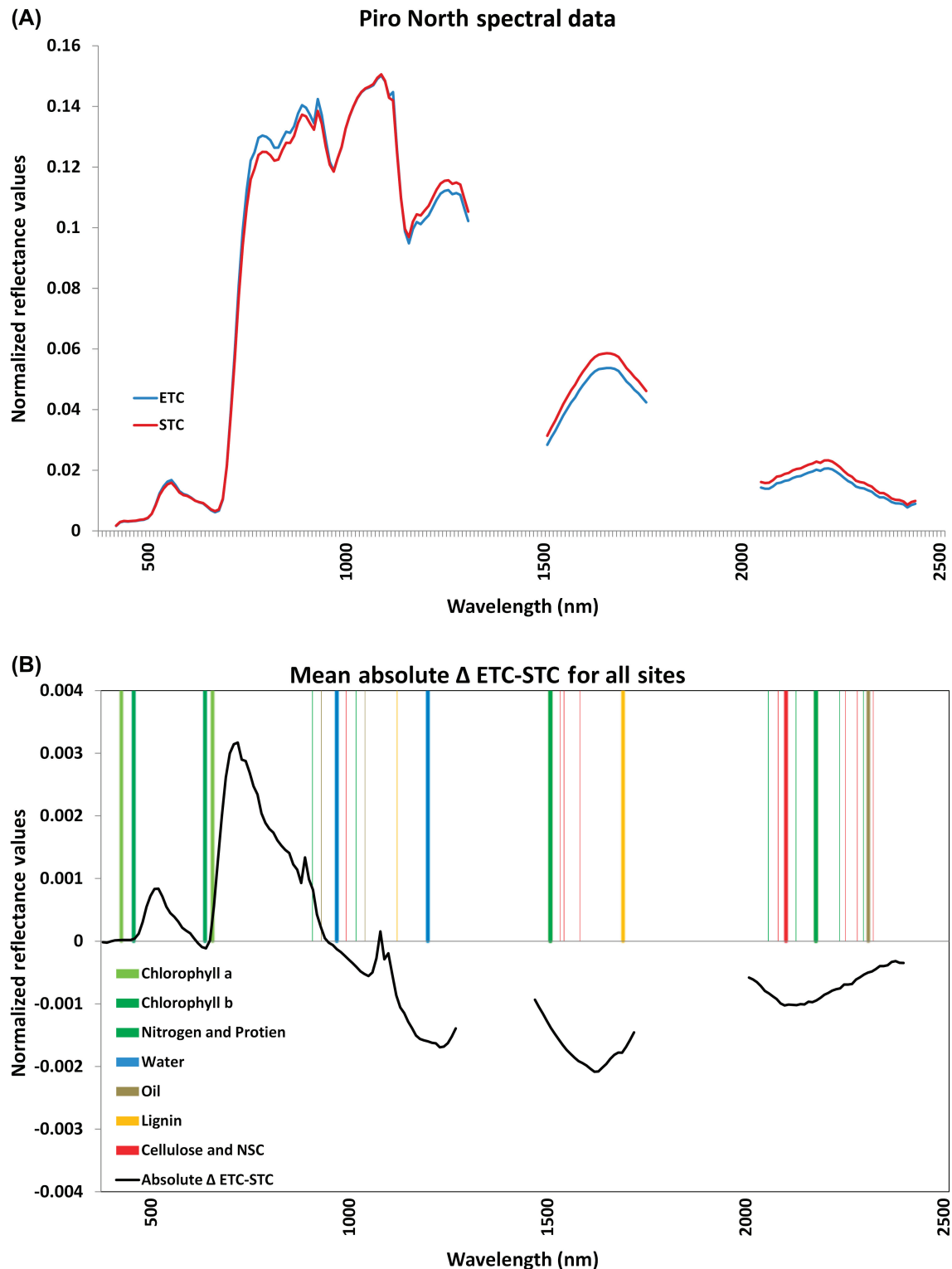
Figure 5. (A) Example spectral data of normalized reflectance at the Piro North landscape. (B) Absolute spectral difference between tall top-of-canopy > 45 m (emergent tree crowns; ETC) and surrounding top-of-canopy between 10–45 m (surrounding tree crowns; STC). The colored bars represent commonly cited elemental and molecular absorption wavelengths. Thicker bands represent elements that have dominant absorption at the given wavelength. The abbreviation, NSC = non-structural carbohydrates. Element absorption data was obtained from Curran (1989) and Asner (2004).

(Montgomery and Chazdon 2002, King et al. 2005, Coonen and Sillett 2015); however, few studies have thoroughly investigated this possibility within tropical forests, due to

challenges of mapping gradients in light with tree growth and size. One study at Barro Colorado Island, Panama, found that light availability and size explained only about 12% of
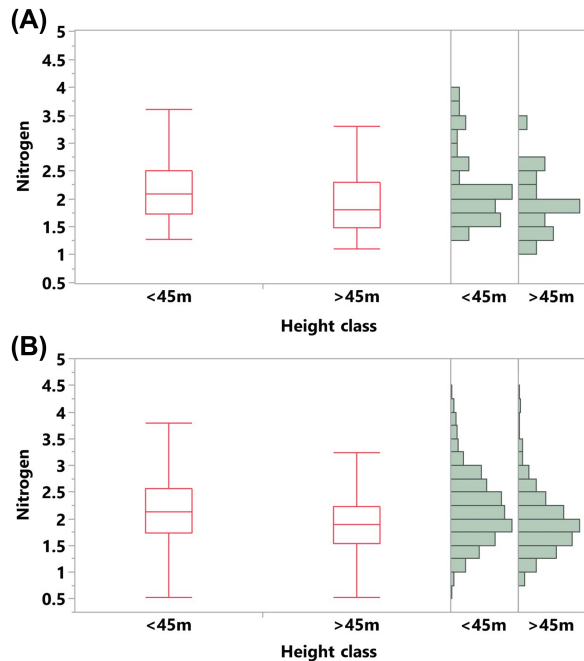
Figure 6. Differences in foliar N (%) concentration by mass between tall top-of-canopy >45 m (emergent tree crowns; ETC) and surrounding top-of-canopy between 10–45 m (surrounding tree crowns; STC). (A) Remotely sensed foliar N ($p < 0.001$). (B) Field collected foliar N ($p < 0.05$).

the variation in wood growth, though 90% of the species showed a positive response to light availability (Rüger et al. 2011). The unexplained variation in tree growth may owe to factors discussed above, and or species-specific strategies that maximize fitness and reproduction. The long-term, evolutionary optimization of life history strategies is expressed in the tremendous functional trait diversity of tropical forests (Asner and Martin 2011) and canopy traits provide clues to biogeographic patterns of species and biogeochemical cycles (Asner et al. 2015b).

Differences in life-history strategies that operate at the scale of the whole organism are often expressed in leaf chemistry and structure, the locus of C fixation and resource investment. In this study, the spectral signature of emergent tree leaves differed from the surrounding lower trees. The observed spectral profile of ETC showed reduced absorption in the NIR, and increased absorption in the SWIR compared to STC (Fig. 5). These differences broadly indicate that emergent trees share leaf morphological and or chemical traits that differ from the STC. This supports prior research that demonstrates morphological and chemical consistency among leaves of taller trees (Kenzo et al. 2012). These shifts in the spectra, such as at the 'red-edge' (680–780 nm) and wavelengths 1510 nm and 2180 nm, are specifically associated with foliar N concentration (Fig. 5B). This pattern of lower canopy N found in the remotely sensed data was paralleled in the field collected data, corroborating that emergent trees generally have lower foliar N content.

The reasons for lower canopy N in emergent trees compared to surrounding canopy is unclear, yet at the species level, it may represent a decline in biomass growth per unit of mass of photosynthetic tissue (growth efficiency), due

to size and age in the taller trees (Sillett et al. 2015a). This decline in efficiency does not necessarily result in an overall reduction in biomass of the trees (Koch et al. 2015, Sillett et al. 2015a, b), but may represent a reallocation of resources and a decrease in foliar N content.

The reduced N at the scale of the forest stand could also reflect differences in species composition and life history strategies between species able to emerge from the canopy and the surrounding trees. Whether foliar N concentrations reflect an active life history strategy or passively track investment in defense compounds is unclear, and warrants future research. A combination of more intensive tree-level sampling of phylogeny, age, structure, biomass and foliar biogeochemistry in conjunction with LiDAR and Hyperspectral data could lead to more insight into the mechanisms driving the observed canopy foliar N patterns.

Regardless of mechanism, the comparatively lower canopy N of emergent trees falls within the theoretical expectation of resource economics spectrum, which broadly posits that plant traits for living long and growing slow are expressed at the cost of rapid growth and reproduction (Reich 2014). More research is needed at the landscape scale to understand how life history strategy and canopy chemical diversity are shaped by environmental factors and phylogenetic diversity. Exploring how the functional biogeography of plant traits stratifies across topographically diverse gradients of resource availability provides a bridge to mechanistically link forest structure to function. This knowledge will improve our understanding of the sensitivity of tropical rainforests to future environmental change, because resource tradeoffs that underlie trait differentiation drive how carbon and nutrients cycle within ecosystems.

References

Aiba, S. and Kitayama, K. 1999. Structure, composition and species diversity in an altitude-substrate matrix of rainforest tree communities on Mount Kinabalu, Borneo. – Plant Ecol. 140: 139–157.

Allen, C. D. et al. 2010. A global overview of drought and heat-induced tree mortality reveals emerging climate change risks for forests. – For. Ecol. Manage. 259: 660–684.

Asner, G. P. 2004. Biophysical remote sensing signatures of arid and semiarid ecosystems. – In: Ustin, S. L. (ed.), Remote sensing for the Earth sciences, 3rd ed. John Wiley and Sons, pp. 53–109.

Asner, G. P. and Martin, R. E. 2011. Canopy phylogenetic, chemical and spectral assembly in a lowland Amazonian forest. – New Phytol. 189: 999–1012.

Asner, G. P. et al. 2007. Carnegie Airborne Observatory: in-flight fusion of hyperspectral imaging and waveform light detection and ranging for three-dimensional studies of ecosystems. – J. Appl. Remote Sens. 1: 013536.

Asner, G. P. et al. 2011. Spectroscopy of canopy chemicals in humid tropical forests. – Remote Sens. Environ. 115: 3587–3598.

Asner, G. P. et al. 2012. Carnegie Airborne Observatory-2: increasing science data dimensionality via high-fidelity multi-sensor fusion. – Remote Sens. Environ. 124: 454–465.

Asner, G. P. et al. 2014. Amazonian functional diversity from forest canopy chemical assembly. – Proc. Natl Acad. Sci. USA 111: 5604–5609.

Asner, G. P. et al. 2015a. Quantifying forest canopy traits: Imaging spectroscopy versus field survey. – Remote Sens. Environ. 158: 15–27.

Asner, G. P. et al. 2015b. Landscape biogeochemistry reflected in shifting distributions of chemical traits in the Amazon forest canopy. – Nat. Geosci. 8: 567–573.

Barrantes, G. et al. 1999. Evaluación de los planes de manejo forestal autorizados en el período 1997–1999 en la Peninsula de Osa. – Cumplimiento de normas técnicas, ambientales e impacto sobre el bosque natural.

Buchs, D. M. et al. 2009. Late Cretaceous to Miocene seamount accretion and melange formation in the Osa and Burica Peninsulas (southern Costa Rica): episodic growth of a convergent margin. – Geol. Soc. Spec. Publ. 328: 411–456.

Chen, Z. S. et al. 1997. Relations of soil properties to topography and vegetation in a subtropical rain forest in southern Taiwan. – Plant Ecol. 132: 229–241.

Clark, D. B. and Clark, D. A. 1996. Abundance, growth and mortality of very large trees in neotropical lowland rain forest. – For. Ecol. Manage. 80: 235–244.

Cleveland, C. C. et al. 2011. Relationships among net primary productivity, nutrients and climate in tropical rain forest: a pan-tropical analysis. – Ecol. Lett. 14: 939–947.

Cochrane, M. A and Laurance, W. F. 2008. Synergisms among fire, land use, and climate change in the Amazon. – Ambio 37: 522–527.

Coonen, E. J. and Sillett, S. C. 2015. Separating effects of crown structure and competition for light on trunk growth of *Sequoia sempervirens*. – For. Ecol. Manage. 358: 26–40.

Cornejo, X. et al. 2012. Phytogeography of the trees of the Osa Peninsula, Costa Rica. – Brittonia 64: 76–101.

Curran, P. J. 1989. Remote sensing of foliar chemistry. – Remote Sens. Environ. 30: 271–278.

Del Grosso, S. 2008. Global potential net primary production predicted from vegetation class, precipitation, and temperature. – Ecol. Soc. Am. 89: 2117–2126.

Detto, M. et al. 2013. Hydrological networks and associated topographic variation as templates for the spatial organization of tropical forest vegetation. – PLoS One 8: e76296.

Doughty, C. E. et al. 2014. Allocation trade-offs dominate the response of tropical forest growth to seasonal and interannual drought. – Ecology 95: 2192–2201.

England, J. R. and Attiwill, P. M. 2006. Changes in leaf morphology and anatomy with tree age and height in the broadleaved evergreen species, *Eucalyptus regnans* F. Muell. – Trees 20: 79–90.

Feilhauer, H. et al. 2010. Brightness-normalized partial least squares regression for hyperspectral data. – J. Quant. Spectrosc. Radiat. Transf. 111: 1947–1957.

Fichtler, E. et al. 2003. Age and long-term growth of trees in an old-growth tropical rain forest, based on analyses of tree rings and 14C1. – Biotropica 35: 306–317.

Fladeland, M. M. et al. 2003. Landscape variations in understory PAR for a mixed deciduous forest in New England, USA. – Agric. For. Meteorol. 118: 137–141.

Fyllas, N. M. et al. 2009. Basin-wide variations in foliar properties of Amazonian forest: phylogeny, soils and climate. – Biogeosciences 6: 2677–2708.

Haaland, D. M. and Thomas, E. V. 1988. Partial least-squares methods for spectral analyses. 1. Relation to other quantitative calibration methods and the extraction of qualitative information. – Anal. Chem. 60: 1193–1202.

Hofhansl, F. et al. 2014. Sensitivity of tropical forest aboveground productivity to climate anomalies in SW Costa Rica. – Global Biogeochem. Cycles 28: 1437–1454.

Holdridge, L. 1967. Life zone ecology. – Tropical Science Center.

Homeier, J. et al. 2010. Tree diversity, forest structure and productivity along altitudinal and topographical gradients in a species rich Ecuadorian montane rain forest. – Biotropica 42: 140–148.

Jenness, J. et al. 2013. Land facet corridor designer: extension for ArcGIS. – Jenness Enterprises, <www.jennessent.com/arcgis/land_facets.htm>.

Kenzo, T. et al. 2012. Variations in leaf photosynthetic and morphological traits with tree height in various vree species in a cambodian tropical dry evergreen forest. – Japan Agric. Res. Q. 46: 167–180.

King, D. A. 1990. The adaptive significance of tree height. – Am. Nat. 135: 809–828.

King, D. A. et al. 2005. The contribution of interspecific variation in maximum tree height to tropical and temperate diversity. – J. Trop. Ecol. 22: 11.

Koch, G. W. et al. 2015. Growth maximization trumps maintenance of leaf conductance in the tallest angiosperm. – Oecologia 177: 321–331.

Laurance, W. F. et al. 2000. Conservation: rainforest fragmentation kills big trees. – Nature 404: 836.

Lindenmayer, D. B. et al. 2012. Global decline in large old trees. – Science 338: 1305–1306.

Lindenmayer, D. B. et al. 2014. New policies for old trees: averting a global crisis in a keystone ecological structure. – Conserv. Lett. 7: 61–69.

Luizão, R. C. C. et al. 2004. Variation of carbon and nitrogen cycling processes along a topographic gradient in a central Amazonian forest. – Global Change Biol. 10: 592–600.

Mascaro, J. et al. 2011. Controls over aboveground forest carbon density on Barro Colorado Island, Panama. – Biogeosciences 8: 1615–1629.

Midgley, J. J. 2003. Is bigger better in plants? The hydraulic costs of increasing size in trees. – Trends Ecol. Evol. 18: 5–6.

Montgomery, R. A. and Chazdon, R. L. 2002. Light gradient partitioning by tropical tree seedlings in the absence of canopy gaps. – Oecologia 131: 165–174.

Nepstad, D. C. et al. 2007. Mortality of large trees and lianas following experimental drought in an amazon forest. – Ecology 88: 2259–2269.

Newbery, M. and Proctor, J. 1984. Ecological studies in four contrasting lowland rain forests in Gunung Mulu national park, Sarawak: IV. Associations between tree distribution and soil factors. – Ecology 72: 475–495.

Niinemets, Ü. 2002. Stomatal conductance alone does not explain the decline in foliar photosynthetic rates with increasing tree age and size in *Picea abies* and *Pinus sylvestris*. – Tree Physiol. 22: 515–535.

Niinemets, U. et al. 2001. Site fertility and the morphological and photosynthetic acclimation of *Pinus sylvestris* needles to light. – Tree Physiol. 21: 1231–1244.

Niklas, K. J. 2007. Maximum plant height and the biophysical factors that limit it. – Tree Physiol. 27: 433–440.

Oliveira, M. A. et al. 2008. Profound impoverishment of the large-tree stand in a hyper-fragmented landscape of the Atlantic forest. – For. Ecol. Manage. 256: 1910–1917.

Passalacqua, P. et al. 2010. A geometric framework for channel network extraction from lidar: nonlinear diffusion and geodesic paths. – J. Geophys. Res. 115: 1–18.

Phillips, O. L. et al. 2010. Drought–mortality relationships for tropical forests. – New Phytol. 187: 631–646.

Porder, S. et al. 2005. Ground-based and remotely sensed nutrient availability across a tropical landscape. – Proc. Natl Acad. Sci. USA 102: 10909–10912.

Porder, S. et al. 2007. Uplift, erosion, and phosphorus limitation in terrestrial ecosystems. – Ecosystems 10: 158–170.

Quesada, C. A. et al. 2012. Basin-wide variations in Amazon forest structure and function are mediated by both soils and climate. – Biogeosciences 9: 2203–2246.

Reich, P. B. 2014. The world-wide "fast-slow" plant economics spectrum: a traits manifesto. – J. Ecol. 102: 275–301.

Rüger, N. et al. 2011. Growth strategies of tropical tree species: disentangling light and size effects. – PLoS One 6: e25330.

Ryan, M. G. and Yoder, B. J. 1997. Hydraulic limits to tree height and tree growth: what keeps trees from growing beyond a certain height? – Bioscience 47: 235–242.

Schuur, E. A. and Matson, P. A. 2001. Net primary productivity and nutrient cycling across a mesic to wet precipitation gradient in Hawaiian montane forest. – Oecologia 128: 431–442.

Sillett, S. C. et al. 2015a. Biomass and growth potential of *Eucalyptus regnans* up to 100 m tall. – For. Ecol. Manage. 348: 78–91.

Sillett, S. C. et al. 2015b. How do tree structure and old age affect growth potential of california redwoods? – Ecol. Monogr. 85: 181–212.

Sist, P. et al. 2014. Large trees as key elements of carbon storage and dynamics after selective logging in the eastern Amazon. – For. Ecol. Manage. 318: 103–109.

Takyu, M. et al. 2002. Effects of topography on tropical lower montane on Mount Kinabulu, Borneo. – Plant Ecol. 159: 35–49.

Takyu, M. et al. 2003. Changes in biomass, productivity and decomposition along topographical gradients under different geological conditions in tropical lower montane forests on Mount Kinabalu, Borneo. – Oecologia 134: 397–404.

Tanner, E. V. J. 1977. Four montane rain forests of Jamaica: a quantitative characterization of the floristics, the soils and the foliar mineral levels, and a discussion of the interrelations. – J. Ecol. 65: 883–918.

Tateno, R. and Takeda, H. 2003. Forest structure and trees species distribution in relation to topography-mediated heterogeneity of soil nitrogen and light at the forest floor. – Ecol. Res. 18: 559–571.

Taylor, P. et al. 2015. Landscape-scale controls on aboveground forest carbon stocks on the Osa Peninsula, Costa Rica. – PLoS One 10: e0126748.

Thomas, R. Q. et al. 2013. Low mortality in tall tropical trees. – Ecology 94: 920–929.

Violle, C. et al. 2014. The emergence and promise of functional biogeography. – Proc. Natl Acad. Sci. USA 111: 13690–13696.

Vitousek, P. et al. 2003. Erosion and the rejuvenation of weathering-derived nutrient supply in an old tropical landscape. – Ecosystems 6: 762–772.

Vitousek, P. M. et al. 2010. Terrestrial phosphorus limitation: mechanisms, implications, and nitrogen-phosphorus interactions. – Ecol. Appl. 20: 5–15.

Wagner, F. et al. 2014. Pan-tropical analysis of climate effects on seasonal tree growth. – PLoS One 9: 20–22.

Wanek, W. et al. 2008. Primary production and nutrient cycling in lowland rainforests of the Golfo Dulce region. – Austria Biol. der Landesmuseen 80: 155–177.

Webb, E. L. et al. 1999. Effects of topography on rainforest tree community structure and diversity in American Samoa, and implications for frugivore and nectarivore populations. – J. Biogeogr. 26: 887–897.

Weintraub, S. R. et al. 2015. Topographic controls on soil nitrogen availability in a lowland tropical forest. – Ecol. Soc. Am. 96: 1561–1574.

Whittaker, R. 1972. Evolution and measurement of species diversity. – Taxon 21: 213–251.

Wright, S. J. et al. 2011. Potassium, phosphorus, or nitrogen limit root allocation, tree growth, or litter production in a lowland tropical forest. – Ecology 92: 1616–1625.

Supplementary material (Appendix ECOG-02062 at <www.ecography.org/appendix/ecog-02062>). Appendix 1.